INTERNATIONAL JOURNAL OF ADVANCE RESEARCH, IDEAS AND INNOVATIONS IN TECHNOLOGY

ISSN: 2454-132X
Impact Factor: 6.078
(Volume 10, Issue 2 - V10I2-1150)
Available online at: https://www.ijariit.com

3D Dense CNN for Hyperspectral Imaging-Based Bloodstain Classification

Tejaskumar B. Sheth
199999915522@gtu.edu.in
Gujarat Technological University, Gandhinagar, Gujarat

Dr. Milind S.Shah
Shah_milind@gtu.edu.in
Shantilal Shah Engineering College, Bhavnagar, Gujarat

ABSTRACT

Blood is a crucial piece of evidence in forensic science for reconstructing and solving crimes. Although numerous chemical procedures are utilized to recognize the blood at a crime scene, these various chemical-based methods might affect DNA analysis. One potential application of bloodstain detection and classification using hyperspectral imaging (HSI) is in forensic science for crime scene investigation. In this paper, we developed a deep learning classifier 2D CNN, 3D CNN and Dense for blood stain detection in the field of forensic science. We conduct experiments using a publicly available Hyperspectral-based Bloodstain dataset for experimental and validation purposes. This dataset contains a variety of chemicals, including blood and blood-like compounds such as ketchup, artificial blood, beetroot juice, poster paint, tomato concentrate, acrylic paint, and questionable blood. With the initial training/testing ratio set to 90/10 of the data samples, we compare the results with state-of-the-art three different CNN architecture with PCA, as preprocessing techniques. The result demonstrates that the 3D Dense CNN can offer improved classification accuracies, smoother classification maps, and more discriminable features for hyperspectral image classification.

Keywords: *Deep Learning, Convolution Neural Network, Dense CNN, Hyperspectral Image Classification, Forensic science, Blood Detection.*

1. Introduction

Since the 1980s, hyperspectral imaging technology has been available. Hyperspectral image (HIS) was originally designed for remote sensing applications that used satellite imaging data of the Earth in land cover mapping, environmental monitoring, agricultural & forestry, with other fields(1). Recent developments in portable HSI technology offer the added potential for this abundance of information on spectral and spatial distributions, which has enabled numerous applications in fields as diverse as pharmaceuticals, detecting and analysing human materials in the environment to aid in emergency response, medical diagnostics , and water resources and flood management (2). Among these crime scene investigations for human body fluids is one. Through the development of fast scanning systems, investigators can scan a scene in a fraction of the time, helping to reduce the workload in forensic laboratories and gain valuable information quickly.

HSI is appropriate for non-contact identification of evidence, reducing the risk of contamination and trace destruction. HSI combines conventional imaging and spectroscopy to produce a three-dimensional data set containing both spatial and spectral information of a crime scene(3).

Human blood detection and identification are critical in crime scene investigations. A variety of techniques are available for this purpose, including chemical enhancement techniques and the use of light sources with 15-30nm bandwidths, which increase the contrast between a trace and its background. Many of these techniques, however, are either destructive or subject to human interpretation. Although various chemical-based blood identification techniques produce excellent results, but they damage blood samples collected from crime scenes, rendering them unusable for DNA extraction or retesting(4).

HSI is similar to a stack of images, each acquired at a specific spectral band. HSI, like spectroscopy, is available in various range of the electromagnetic spectrum, such as ultraviolet (UV), visible (Vis), near infrared (NIR), mid infrared (IR), and even thermal infrared. Reflected spectra with resolutions as low as 10nm can be treated as miniature spectrographs. whereas spatial resolutions can vary depending on the application(5).

Human blood has distinct spectral characteristics that can be identified in hyperspectral data. Haemoglobin is the main component in blood that absorbs and scatters light in a characteristic manner, resulting in distinct absorption features in the visible and near-infrared (NIR) regions of the electromagnetic spectrum. By examining the spectral reflectance of different pixels in the image across various wavelengths, it is possible to detect the presence of blood.

The advantages of using HIS in-crime scene investigation include faster data acquisition, reduce need of trained laboratory technician, no specimen preparation, reduced human error, no trace destruction, no specimen preparation, and the ability to produce consistent visual results.

The remaining sections of this paper are structured as follows: Section 2 discusses the related work, and Section 3 provides the details of the proposed 2D CNN, 3D CNN and 3D Dense CNN classification network, including the description of the dataset used in the experiment. Section 4 presents the experimental results and analysis, while Section 5 concludes the paper.

2. Related Work

Bloodstain identification is a crucial aspect of forensic investigation at a crime scene. Over the time various non-contact, non-destructive techniques have been used. Different spectroscopic techniques such as Raman, Reflectance, Electron Paramagnetic Resonance (EPR), Nuclear Magnetic Resonance (NMR), and Infrared (IR) spectroscopies such as Attenuated Total Reflectance Fourier Transform IR spectroscopy (ATR-FTIR) are used by practitioners. For bloodstain identification, IR and Raman-based techniques yield promising results (6).

All of these spectroscopy techniques are used the spectral information of bloods and did not consider spatial information or image area under observation. Irrespective of the various spectroscopy methodologies above, The HSI technique is an excellent technique that extracts from a specimen both spectral and spatial information, producing a three-dimensional data set. It combines the spectroscopy technique with conventional imaging, obtaining hyperspectral images by measuring numerous narrow wavelength regions with high resolution.

In the early days of research work for HSI classification, the main focus was on exploring spectral signatures of individual items present in HSIs can be classified using pixel-wise classification methods like support vector machines (SVM) logistic regression (LR). Furthermore, because HSIs have a high dimension, various feature extraction and dimension reduction methods, such as principal component analysis (PCA), improve classification accuracies(7). However, classification accuracies were not satisfactory until spatial and spectral information were factored into classification methods. Lately, spatial information has been incorporated along with spectral information and is reported to be quite helpful in improving the classification accuracies in many approaches. Recent success in implementing complex (>2 layer) artificial neural networks (ANN) for image classification opens doors for HSI classification using various deep learning methods(8).

In (9) the paper introduces the Dense Convolutional Network (DenseNet) architecture, which connects each layer to every other layer in a feed-forward fashion, resulting in L(L+1)/2 direct connections. This dense connectivity pattern is achieved by concatenating the feature-maps of all preceding layers as inputs to each layer and using the layer's own feature-maps as inputs to all subsequent layers. This dense connectivity pattern strengthens feature propagation, encourages feature reuse, and reduces the number of parameters.

In(10) the paper proposes a non-destructive method for bloodstain identification using Hyperspectral Imaging (HSI) in the 397-1000 nm range. The method is based on the visualization of home-components bands in the 500-700 nm spectral range. Five different classifiers (SVM, ANN, KNN, Random Forest, and Decision Tree) were trained using important spectral bands selected from the derivative spectrum. The comparative analysis reveals that the proposed method outperformed several state-of-the-art methods.

In (11) author compare the performance of different deep learning architectures 1D CNN, 2D CNN, 3D CNN, RNN with baseline results of Support Vector Machine (SVM) to identify the bloodstain. The various deep learning method shows 74-94% accuracy with training and testing sample of 75-25%.

In our work we implemented 2D CNN, 3D CNN and Dense CNN for comparison and classification of bloodstain. The 2D CNN, 3D CNN architecture was reimplemented from paper (11) and Dense CNN architecture was reimplemented form paper (9). The PCA and block size with learning and testing environment parameter were set common for all three models.

3. Methodology

Let's denote an HSI cube ($X \in R$, $H \times W \times B$). Where H and W are the height and width of the spatial dimensions, respectively, and B is the number of spectral bands. To represent various blood and blood-like substances, a one-hot label vector $Y = (y_1, y_2,..., y_C) \in R\ 1\times1\times C$ is employed, where C represents the total number of categories.

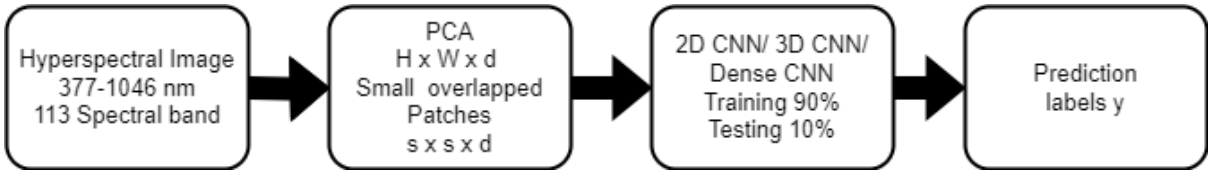

Figure 1 Framework for HSI classification.

Figure 1 *Framework for HSI* depicts the implemented framework for HSI classification. In the spectral dimension, the principal component analysis (PCA) algorithm is used to reduce dimensionality and extract the most informative components. Because CNN requires both spectral and spatial information, the HSI cube is cropped into small, overlapped patches as samples. Finally, a 2D CNN, 3D CNN and Dense CNN modules implemented to extracts 3-D feature graphs from image patches and assigns each pixel to one of the classes.

2D CNN

2D Convolution Neural Network (2DCNN) is made up of three 2D convolution layers, one flatten layer, and two fully linked layers The ReLU activation function is used by all three 2D convolution layers as well as the first fully linked layer. The final fully linked neural network used the SoftMax activation function.

3D CNN

3D Convolution Neural Network (3DCNN) is made up of three 3D convolution layers, one flatten layer, and two fully linked layers. The ReLU activation function is used by all three 3D convolution layers as well as the first fully linked layer. The final fully linked neural network used the SoftMax activation function.

3D Dense CNN

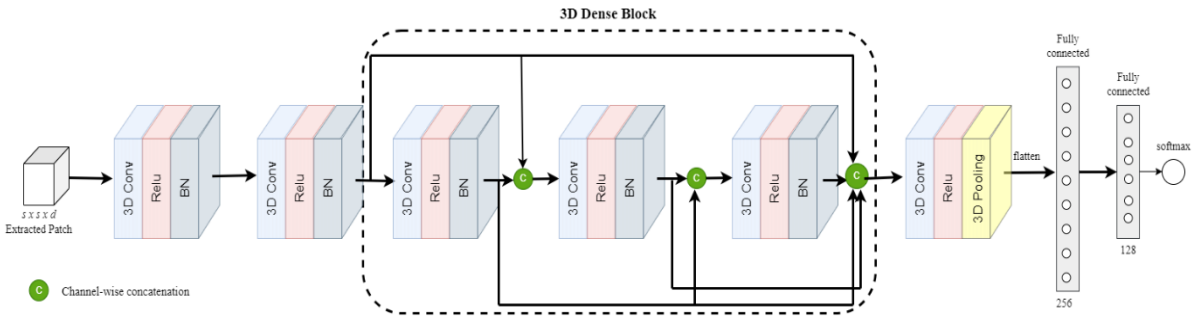

Figure 2 Displays the proposed and implemented 3D dense CNN framework for HSI

Our CNN design is based on 3D CNN and has dense connectivity. 3D Dense CNN proposed implemented farmwork is shown in Figure 2. Our model's first three layers are 3-D convolutional layers, with 8 convolutional kernels of dimension 3 x 3 x 5 for the al3-D input. Next, three 3-D convolutional layers with dense connections

are added. Three-dimensional convolution layers with 16 filters are utilised throughout, with a kernel size of 3 x 3 x 3. Batch normalisation is used after each 3D convolution to regularise the learning process and prevent overfitting. The final convolution layer block includes 16 filters and a kernel size of 1 x 1 x 1, followed by 3-D pooling.

Finally, the 3D cubes are flattened into classes. Finally, the 3-D feature cubes are flattened to 1-D, and the flatten layer is mapped to the number of classes via two fully connected layers. Dropout is used in completely connected layers. The activation function is rectified linear units (ReLUs) after each convolution layer, and the optimizer 'Adam' is used to optimise the soft-max loss function once the final fully linked layers are employed.

Bloodstain Detection Dataset

Our experiments make use of hyperspectral images from the dataset described in (12) which is freely available to the public under an open licence (the dataset can be assessed from https://zenodo.org/record/3984905).The dataset used in this paper has hyperspectral images of six different parts of one mock-up crime scene. The latter A-F are used to identify the different HSI frame as shown in Figure 3.

(a)The mock-up of a forensic scene with locations of images A-F

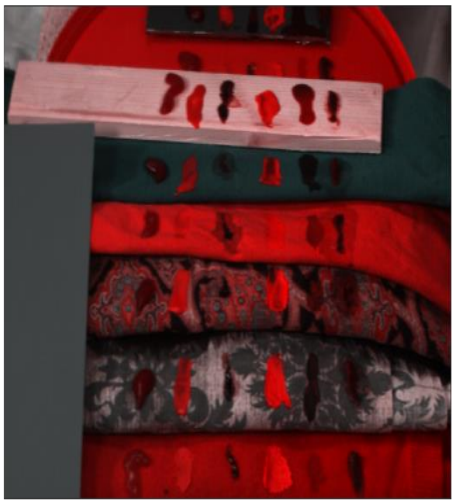

(b) RGB rendering of Image E(I)

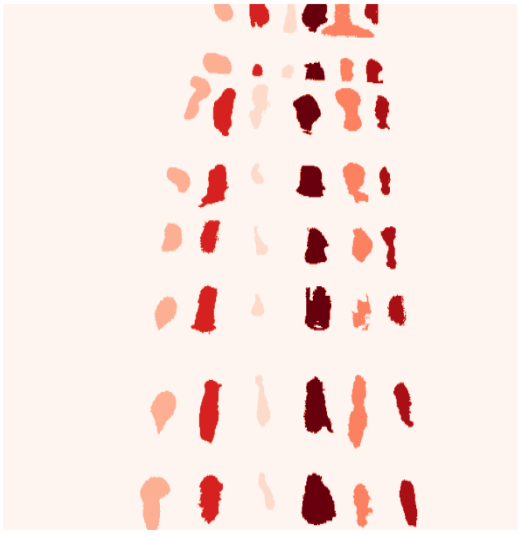

(c) Ground truth of image E(I)

Figure 3: Illustration of the dataset

Out of the six different images of the mock-up scene E, 'Comparison', is chosen for the experiment in this paper. Scene-E 'Comparison' RGB rendering image and its ground truth image are shown in Figure 3 (b) and Figure 1(c) respectively. In the scene-E, a trace of real blood and bloods look alike substances with eight different backgrounds is present . Scene-E 'Comparison' has wood, plastic, metal, and some of the red-hued fabric. These materials are arranged in vertical fashion, and blood and blood-like substances are placed horizontally on them. The image provides challenging and diverse environments for finding blood.

4. Experimental Result

We assess the performance of our all three architecture in a hardware environment that includes the Google Colab cloud platform and GPUs. When comparing all three neural network and maintain the majority of environmental elements unchanged. The total dataset is split as 80% for training and 10% for validation. The remaining 10% is treated as a blind set (i.e., test set) for the final model evaluation.

The Adam optimizer was assigned an ideal learning rate of 0.001 and a momentum of 0.9. All convolution layers in each model employ "relu" as an activation function, with the exception of the final layer. The final convolution layer utilised is "softmax". To ensure the validity of the results for various deep learning methods, the HSI cube dimensions of 9 x 9, 11 x 11, and 13 x13 were employed. The model was trained for a total of ten epochs.

To assess the performance of the aforementioned models, we use the overall accuracy (OA), average accuracy (AA), and Kappa coefficient, and we present the averaged findings in Table 1. after ten independent runs in all experiments. The results demonstrate that for given databse the 3D Dense CNN model outperforms all existing approaches. Table 2. Shows bloodstain classification results using 3D Dense CNN when 9 X 9 hyperspectral cube is used with PCA of 75 components. The overall accuracy (OA), precision (P), recall (R), and F1score (F1) are calculated to validate the performance of the proposed 3D Dense CNN model when the mock-up scenario E is used. It achieves 95% total accuracy.

Table 1. Classification Accuracy Using 2DCNN,3DCNN, and 3D Dense, Performance.

Methods	Window								
	9 x 9			11 x 11			13 x 13		
	OA	AA	kapp	OA	AA	kapp	OA	AA	kapp
2DCNN	83.44	82.40	81.55	83.02	83.00	82.01	81.03	81.80	81.67
3DCNN	93.68	91.96	92.96	**93.95**	**92.45**	91.93	90.35	86.71	89.26
DENSE	**94.44**	**95.00**	**93.12**	93.12	92.43	**93.58**	**92.87**	**90.12**	**92.01**

Table 2. Bloodstain Classification Results using A 3D Dense CNN.

Sample	***Precision***	***Recall***	***F1-Score***
Blood	*0.99*	*0.88*	*0.93*
Ketchup	*0.98*	*0.99*	*0.99*
artificial blood	*0.85*	*0.94*	*0.89*
poster paint	*1.00*	*1.00*	*1.00*
tomato concentrate	*0.91*	*0.85*	*0.88*
acrylic paint	*0.98*	*0.97*	*0.97*
Accuracy			*0.95*
Macro avg.	*0.95*	*0.95*	*0.94*
Weighted avg	*0.95*	*0.95*	*0.95*

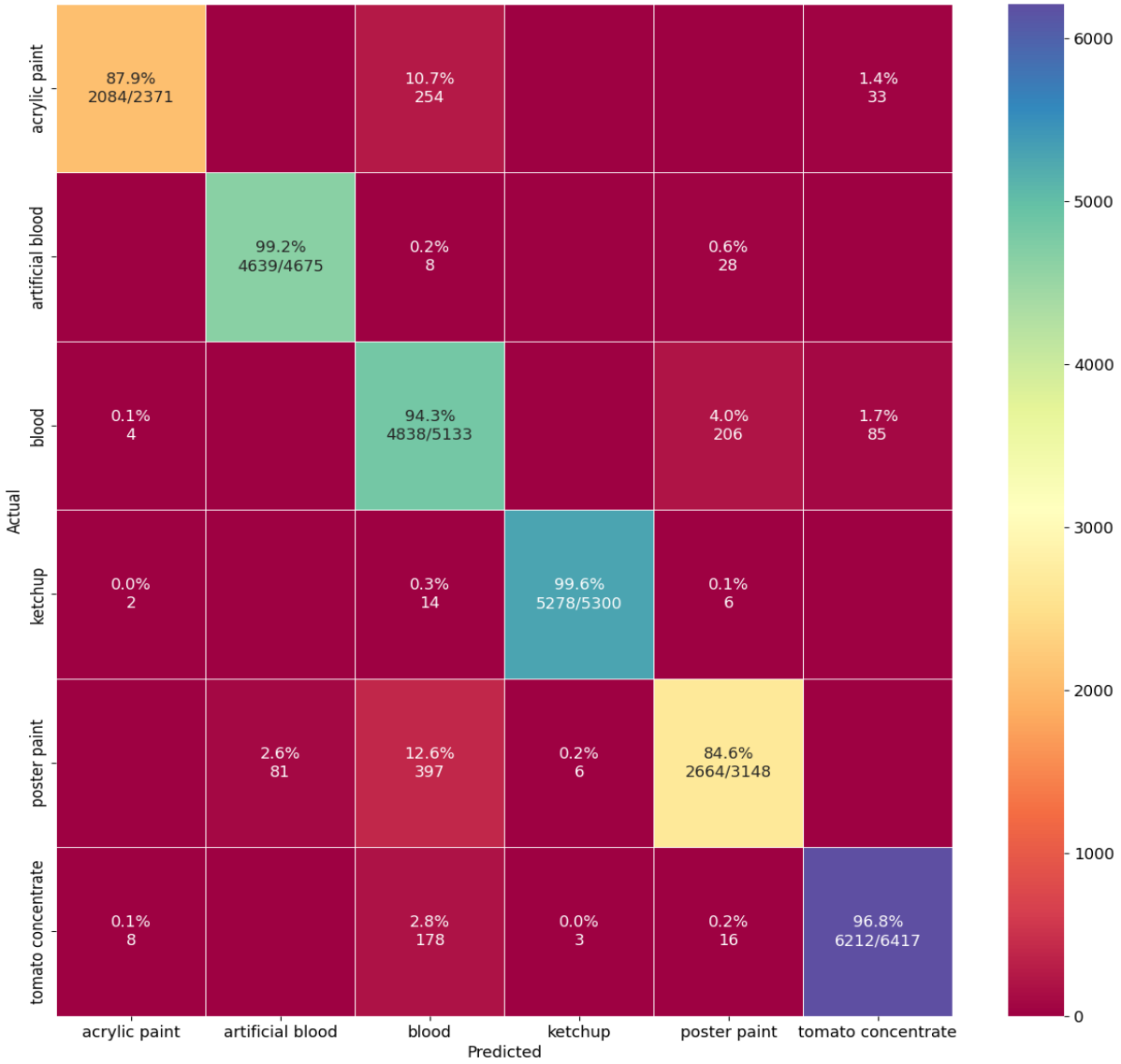

Figure 4. The confusion matrix using 3D Dense CNN Model

(a)

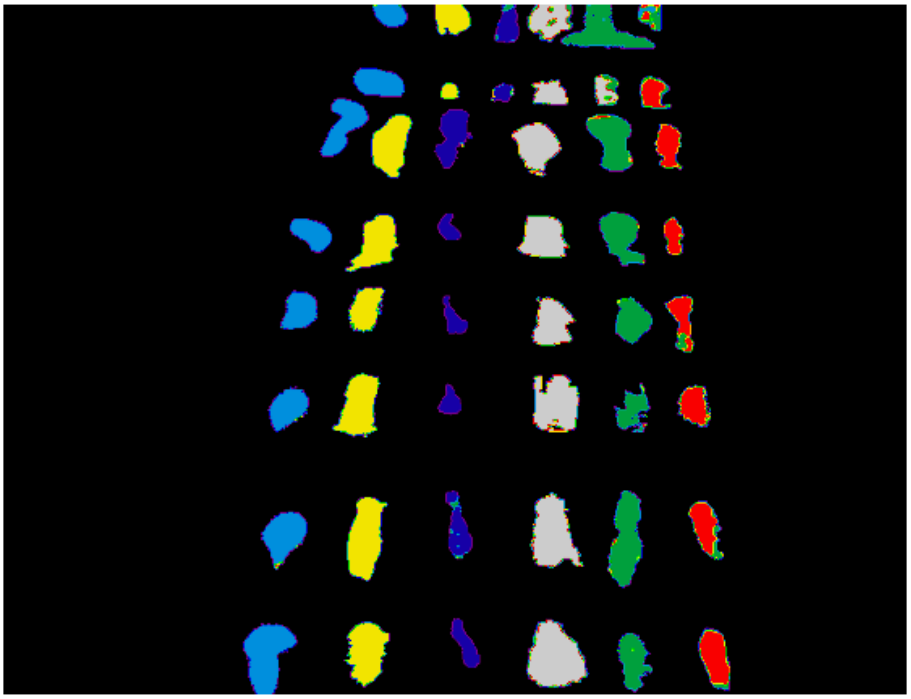

(b)

Figure 5. (a)Original Image frame" scene E" with annotation

(b) predicted Ground Truths using 3D DWT DWNSE CNN model

The performance of the proposed models has been evaluated using confusion matrices of the E scenario, as depicted in Figure 4. The 3D dense CNN method achieves an average accuracy (AA) of 95% in classifying blood traces from other red hues, as depicted in . In addition, Figure 5. displays the classification accuracy for graphical maps (i.e., Ground Truths) attained by the 3D Dense CNN.

5. Conclusion

In this study, three different deep neural networks are implemented to classify blood and blood-look alike compounds in hyperspectral image with different backgrounds.. The installed 2DCNN, 3DCNN, and 3D Dense CNNs could recognise blood samples containing blood-like compounds from mock up crime senses. The total classification accuracy demonstrates that HIS can be used to identify blood at complicated crime scenes without the need for a skilled lab technician or destructive chemical procedures. Among the implemented deep neural network, 3D Dense CNN considerably improved blood strain categorization performance in mock criminal scenarios. 3D Dense CNN can classify blood with a greater accuracy of 95%. The dense connection module can be utilised to optimise CNN classification architecture based on HSI's spectral and spatial dimensions. The experimental findings confirmed the superiority of our technique, which is especially evident when the HSI has many visually comparable categories, a complicated background, and limited number of training samples.

6. References

1. Jia S, Jiang S, Lin Z, Li N, Xu M, Yu S. A survey: Deep learning for hyperspectral image classification with few labeled samples. Neurocomputing [Internet]. 2021 Aug;448:179–204. Available from: https://doi.org/10.1016/j.neucom.2021.03.035

2. Jaiswal G, Sharma A, Yadav SK. Critical insights into modern hyperspectral image applications through deep learning. Wiley Interdiscip Rev Data Min Knowl Discov. 2021;11(6).

3. Williams GA. Forensic Science International : Reports Body fluid identification : A case for more research and innovation. Forensic Sci Int Reports [Internet]. 2020;2(February):100096. Available from: https://doi.org/10.1016/j.fsir.2020.100096

4. Virkler K, Lednev IK. Analysis of body fluids for forensic purposes: From laboratory testing to non-destructive rapid confirmatory identification at a crime scene. Vol. 188, Forensic Science International. 2009. p. 1–17.

5. Schalik R, Illes M. A Review of Spectroscopic Methods Applied to Bloodstain Pattern Analysis. 2019;2(1).

6. Zapata F, Gregório I, García-ruiz C. Body Fluids and Spectroscopic Techniques in Forensics : A Perfect Match ? 2015;1(1):1–7.

7. Uddin MP, Mamun MA, Hossain MA. Feature extraction for hyperspectral image classification. In: 5th IEEE Region 10 Humanitarian Technology Conference 2017, R10-HTC 2017. Institute of Electrical and Electronics Engineers Inc.; 2018. p. 379–82.

8. Wambugu N, Chen Y, Xiao Z, Tan K, Wei M, Liu X, et al. Hyperspectral image classification on insufficient-sample and feature learning using deep neural networks: A review. Int J Appl Earth Obs Geoinf [Internet]. 2021;105:102603. Available from: http://dx.doi.org/10.1016/j.jag.2021.102603

9. Huang G, Liu Z, Van Der Maaten L, Weinberger KQ. Densely Connected Convolutional Networks. In: 2017 IEEE Conference on Computer Vision and Pattern Recognition (CVPR) [Internet]. IEEE; 2017. p. 2261–9. Available from: https://ieeexplore.ieee.org/document/8099726/

10. Zulfiqar M, Ahmad M, Sohaib A, Mazzara M, Distefano S. Hyperspectral Imaging for Bloodstain Identification. Sensors [Internet]. 2021 Apr 27;21(9):3045. Available from: https://www.mdpi.com/1424-8220/21/9/3045

11. Książek K, Romaszewski M, Głomb P, Grabowski B, Cholewa M. Blood Stain Classification with Hyperspectral Imaging and Deep Neural Networks. Sensors [Internet]. 2020 Nov 21;20(22):6666. Available from: https://www.mdpi.com/1424-8220/20/22/6666

12. Romaszewski M, Głomb P, Sochan A, Cholewa M. A dataset for evaluating blood detection in hyperspectral images. Forensic Sci Int [Internet]. 2021 Mar;320:110701. Available from: https://linkinghub.elsevier.com/retrieve/pii/S0379073821000219

